Chemical Bonding in Metallic Rutile-type Oxides TO2 (T = Ru, Rh, Pd, Pt)

Gérard Demazeau, Samir F. Matar, Rainer Pöttgen

Chemical Bonding in Metallic Rutile-type Oxides TO_2 (T = Ru, Rh, Pd, Pt)

Gérard Demazeau[a], Samir F. Matar[a], and Rainer Pöttgen[b]

[a] ICMCB – CNRS, Université Bordeaux 1, 87, Avenue du Docteur A. Schweitzer, 33608 Pessac Cedex, France
[b] Institut für Anorganische und Analytische Chemie, Universität Münster, Corrensstraße 30, D-48149 Münster, Germany

Reprint requests to S. F. Matar. E-mail: matar@icmcb-bordeaux.cnrs.fr

Z. Naturforsch. **2007**, *62b,* 949 – 954; received April 4, 2007

Dedicated to Dr. Bernard Chevalier on the occasion of his 60th birthday

Synthesis routes to rutile-type oxides with 4*d* and 5*d* transition elements are summarized. Trends in electronic structure have been established through an analysis in the framework of density functional theory presenting the band structure, the density of states and the properties of chemical bonding. The metal-oxygen bond is found to play the major role in bonding of the system in the valence band. Throughout the series $4d \rightarrow 5d$ (RuO_2, RhO_2, PdO_2 and PtO_2) the crystal field analysis of the band structure shows a lowering of e_g towards t_{2g} manifolds and a broadening of the overall density of states. In the vicinity of the Fermi level the role of the antibonding metal-oxygen character is investigated in the context of instability towards possible magnetic polarization, especially for RuO_2.

Key words: Oxides, RuO_2, RhO_2, PdO_2, PtO_2, Rutile-type, DFT

Introduction

Twenty years ago Zaanen, Sawatzky and Allen (ZSA) [1] proposed an interesting description of metal oxides taking into account correlation effects. According to this description the electronic properties of oxides can be described in terms of the relative energies of three electronic energy levels near the Fermi level: (i) the energy-level of the oxygen 2*p* states fully occupied, (ii) the energy level of the highest occupied metal orbital, and (iii) the energy level of the lowest unoccupied metal orbital (corresponding to the metal conduction band).

Among the many metal oxides, transition metal dioxides represent an important family of materials due to their physical properties [2]. Besides CrO_2, an important ferromagnetic material for recording tapes, most of the transition metal dioxides are widely used in the field of catalysis. From the 3*d* to the 4*d* transition metal row, due to the increase of the strength of the T^{4+}–O bond, the physical properties of the corresponding oxides are modified. Recently Matar and Campet [3] proposed the so-called '$\chi\eta$ model' which allows predicting the metallic behaviour of an oxide. It is mainly based on simple chemical criteria such as the electronegativity χ and the chemical hardness η. Applying this model, one would expect metallic behaviour for the group including RuO_2, RhO_2, PdO_2 and PtO_2, considered herein. Complementing such models, the support of experimental findings (crystallography, physical data, *etc*.) by band theoretical investigations is of great relevance. For the transition metal 4*d* and 5*d* dioxides this appears to be particularly important in order to evaluate the role of the T^{4+}–O covalence. This is the object of the present work.

Experimental Data on TO_2 Oxides

Ruthenium dioxide appears in nature in the rutile-type structure [4] (Fig. 1). The high-pressure behaviour of RuO_2 was investigated either under static compression [5] or shock compression [6]. Under static compression a first phase transition was observed at 6 GPa from the rutile-type to the orthorhombic $CaCl_2$-type characterized by a slight deformation of the ambient-pressure tetragonal rutile structure. At 12 GPa a second transition from the $CaCl_2$-type to a modified fluorite-type structure with an increase of the cationic coordination number $\{6+2\}$ took place. Using shock com-

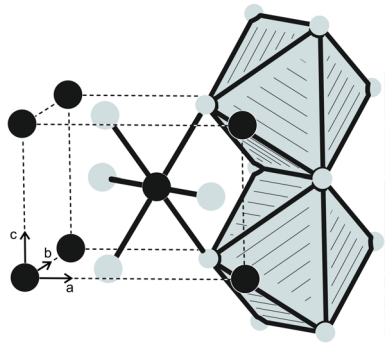

Fig. 1. The rutile-type structure of the dioxides TO_2 (T = Ru, Rh, Pd, Pt). Transition metal and oxygen atoms are drawn as black and light gray circles, respectively. The edge- and corner-sharing $TO_{6/3}$ octahedra are emphasized.

pression only the first transition close to 6 GPa was detected.

Rhodium dioxide was first claimed by Muller and Roy using $Rh_2O_3 \cdot 5H_2O$ as precursor and an oxygen pressure up to 350 MPa [7]. A recent thermogravimetric study of the resulting compound has shown that stabilization by OH groups induces the formation of the rutile-type structure of the compound $[Rh^{4+}_{(1-x)}Rh^{3+}_{x}O_{2-x}OH_x]$. Subsequently, an anhydrous high oxygen pressure synthesis was developed using $RhCl_3$ as a precursor and Na_2O_2 as both oxidant and chloride trapping agent. A structural study has confirmed that RhO_2 adopts the rutile structure with Rh^{4+} in a slightly distorted octahedral coordination of oxygen atoms at Rh–O distances of 1.950 Å (4×) and 1.983 Å (2×) [8].

Palladium dioxide with the rutile structure was claimed by Shaplygin *et al*. [9]. The high-pressure preparation process used PdO as a precursor and thermal decomposition of $KClO_3$ as *in situ* oxygen source in a belt-type equipment (4 GPa, 950 °C). The reproducibility of such a preparative route appears to be difficult due to the low thermal stability of PdO_2.

The preparation of platinum dioxide was first attempted under oxygen pressures (20 – 400 MPa) by Muller and Roy using PtI_2 as starting material [7]. As a function of temperature, two different modifications have been observed: α-PtO_2 and β-PtO_2. The CdI_2-type structure was proposed for the α-form, but due to the poor crystallinity of this oxide, the structure type requires confirmation. Single crystals of β-PtO_2 have been grown from elemental platinum and $KClO_3$ mixtures under high pressures [4 GPa – 1500 °C] in a modified belt-type equipment [10]. The observed orthorhombic space group *Pbnm* confirmed the $CaCl_2$-type structure, an orthorhombically distorted variant of the rutile-type inducing different Pt–O distances ($2 \times 1.989(4)$ and $4 \times 2.003(4)$ Å).

The oxygen x parameter of RhO_2 [8] was used throughout this work as the only variable. All electronic structure computations are fully *ab initio*.

Theoretical Investigations of the Band Structures

Computational framework

Early [11, 12] and more recent [13, and ref. therein] theoretical studies on rutile-type oxides were carried out with the aim of establishing the electronic structure *vs*. chemical bonding relationship. While the early studies focused on a comparison of RuO_2 with TiO_2, VO_2, and CrO_2, herein we report a comparison within the series RuO_2, RhO_2, and PdO_2. Within the framework of the well established density functional theory DFT [14] we used the all electrons augmented spherical wave (ASW) method in a scalar relativistic implementation [15] due to the presence of heavy elements with $Z > 50$. The exchange-correlation effects were accounted for within the generalized gradient approximation (GGA) using the parameterization of Perdew, Burke and Ernzerhof [16]. In the ASW method, the wave function is expanded in atom-centered augmented spherical waves, which are Hankel functions and numerical solutions of Schrödinger's equation, respectively, outside and inside the so-called augmentation spheres. The transition metal *ns*, *np* and $(n-1)d$ states, n = 5 for Ru, Rh, Pd and n = 6 for Pt and O 2*s*, 2*p*, were used for valence basis sets. Further, due to the open nature of the rutile structure, empty spheres (ES) were introduced within the atomic sphere approximation ASA of the ASW method [15]. ES are pseudo atoms with zero atomic numbers and a limited valence basis set like oxygen, so that they receive charges from neighboring atoms and allow for covalence within the structure. A sufficiently large number of k points were used to sample the irreducible wedge of the simple tetragonal Brillouin zone for the plot of the electronic band structure. The energy and charge differences between successive iterations were converged below $\Delta E = 10^{-8}$ Ryd. and $\Delta Q = 10^{-8}$, respectively.

To extract more information about the nature of the interactions between the atomic constituents from electronic structure calculations, the crystal orbital overlap

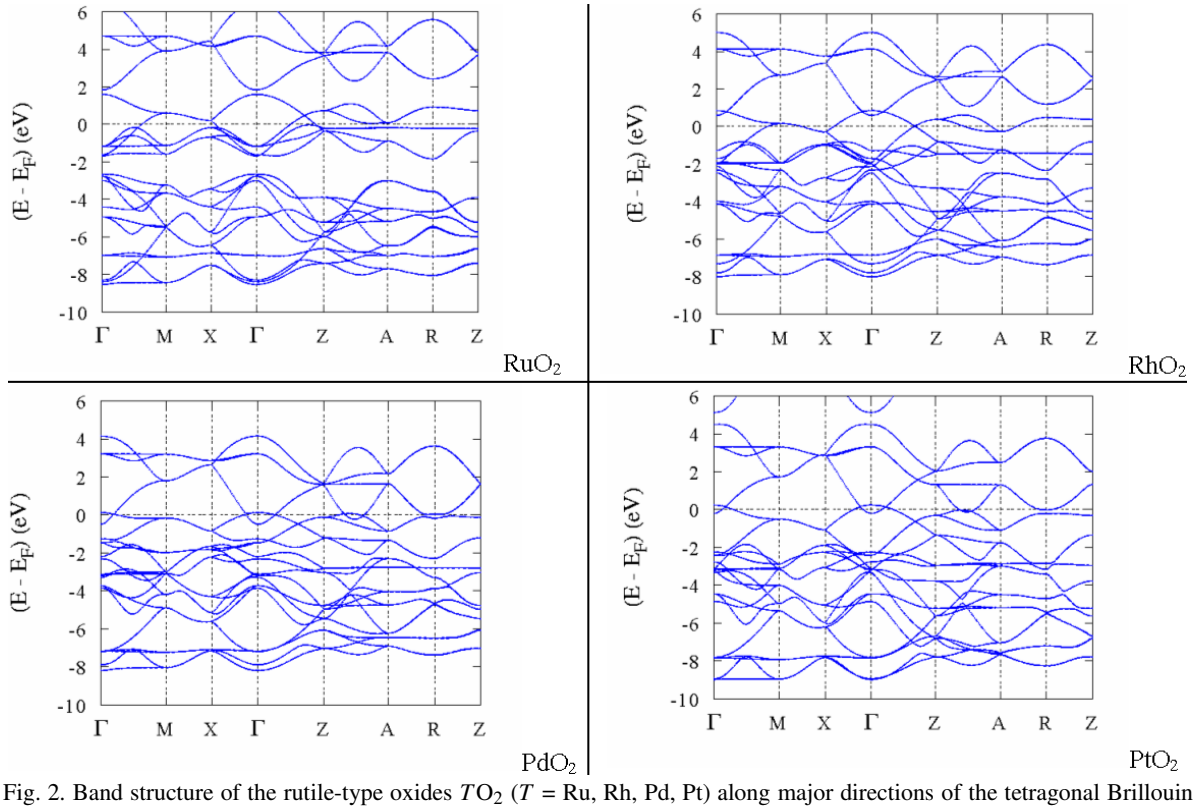

Fig. 2. Band structure of the rutile-type oxides TO_2 (T = Ru, Rh, Pd, Pt) along major directions of the tetragonal Brillouin zone.

population (COOP) [17] or the crystal orbital Hamiltonian population (COHP) [18] can be employed. Both approaches provide a qualitative description of the bonding, nonbonding and antibonding interactions between atoms. A slight refinement of the COHP was recently proposed in the form of the "energy of covalent bond" (ECOV), which combines COHP and COOP to calculate quantities independent of the choice of the zero of potential [13]. Both COOP and ECOV give similar general trends, but COOP, when defined within plane-wave basis sets, exaggerates the magnitude of antibonding states. In the present work the ECOV was used for the chemical bonding analysis. In the plots, negative, positive and zero ECOV magnitudes are relevant to bonding, antibonding and nonbonding interactions, respectively.

Results of the Calculations and Discussion

Band structure

Fig. 2 shows the band structures of the four metal oxide systems plotted along the major directions of the Brillouin zone of the simple tetragonal Bravais lattice. Note that these oxides have 2 formula units per cell (T_2O_4) so that one expects two sets of bands, *i. e.* 2×2 e_g, 2×3 t_{2g} for the d metal and 4×3 p bands for oxygen.

The O_h-like crystal field analysis follows from the simple counting of the bands. From the first panel (RuO_2), looking at the ZA line, one finds the four e_g-like bands by counting 4 dispersion lines from the top of the panel. The e_g bands are all found above E_F and well separated from the six t_{2g}-like bands which are crossed by the Fermi level. In RuO_2, the interesting feature of the flat band in the close neighborhood of the Fermi level should be correlated with an instability of the system when accounted for in the spin degenerate (total spins) configuration such as the one assumed here. This point is further discussed in the DOS section. The oxygen bands are within the valence band and they can be counted to be 12 in number. Along the 4d series (Ru, Rh, Pd) with one electron added up for each step and a larger filling of the d subshell, the trend is towards a smaller energy difference between

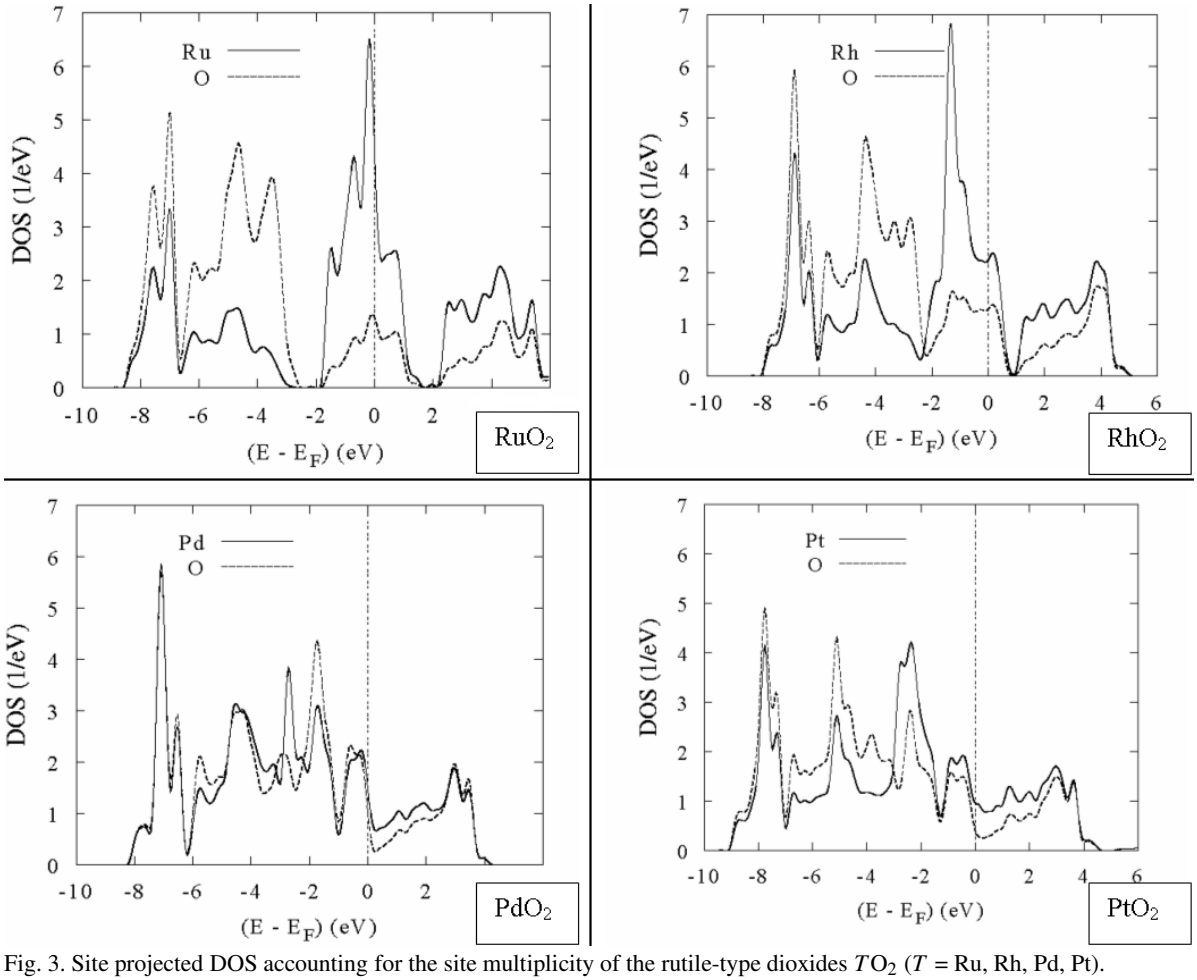

Fig. 3. Site projected DOS accounting for the site multiplicity of the rutile-type dioxides TO_2 (T = Ru, Rh, Pd, Pt).

the different bands (e_g, t_{2g} and p) and a lowering of the e_g bands which are crossed by the Fermi level for T = Pd and Pt; for the latter the bands are no longer separated and one observes just one block of bands. This is a sign of an increased covalence of the bonding upon going from RuO_2 to RhO_2 where e_g and t_{2g} mix together along the ZA line. From Pd to Pt, which are isoelectronic, the trend is the same but with a larger energy window since the Pt(5*d*) bands are broader than the Pd(4*d*) bands.

Density of states

The site projected DOS (PDOS) accounting for site multiplicity within the rutile structure, *i. e.* 2 metals per 4 oxygens, are shown in the four panels of Fig. 3, the energy reference along x being at the Fermi level. For the sake of clarity we do not show the small PDOS contribution arising from the ES. It is sufficient to say that they receive charge residues from both T and O. Due to the crystal orientation used in our calculations, the t_{2g} and e_g manifolds are inclusive of $d_{x^2-y^2}$, d_{xz}, d_{yz}, and d_{xy}, d_{z^2}, respectively. This approach is somewhat different from the usual procedure, but the difference is artificial since the physical concept is the same. From this one can notice that the e_g states are mainly responsible for the DOS within the valence band VB, *i. e.* they secure the bonding with oxygen (see for instance the energy window from -8 to -6 eV), while the t_{2g}-like states are less involved in the bonding and show intense peaks such as at E_F. The different PDOS can be seen to mirror the observations made above with the following trends:

(i) From the first panel showing the RuO_2 plots, both the Ru and O PDOS run alike for the lower (at

ca. −8 eV) and upper part (between 2 and −6 eV) of the panel; this points to the strong σ bonding within the 'TO_6'-like octahedron. The relatively large DOS at the Fermi level for Ru is due to the crossing of the t_{2g} manifold by E_F (see band structure panel). Within the Stoner mean field theory of band ferromagnetism [13], the large DOS at E_F is a sign of a magnetic instability, and as a matter of fact spin-polarized calculations of RuO_2 point to the onset of a small but finite magnetic moment of 0.044 μ_B per Ru atom and a total magnetization of 0.116 μ_B per formula unit. Although former theoretical studies on the electronic structure of RuO_2 [11, 12] pointed to its metallic character, this is the first proposal of weak ferromagnetism in RuO_2. This is unexpected, because 4*d* elements are rarely seen to support a spontaneous magnetic moment. Nevertheless, this could be changed as a result of the experimental conditions of sample preparation (bulk, thin layers…) and needs to be checked experimentally. Moreover this is not significant of a true magnetically ordered system such as CrO_2 formerly studied by us in the same theoretical framework [13]. It needs to be noted here that a large DOS at the Fermi level arising from t_{2g}-like orbitals is correlated with a certain instability of such a non magnetic state. In VO_2, the system "relaxes" to become monoclinic; this translates as a structural instability. In CrO_2 the system relaxes to become a half metallic ferromagnet, and RuO_2 seems to be on the verge of such a magnetic instability.

(ii) Within the series of 4*d* compounds, the *T* metal PDOS at E_F decreases due to the energy lowering of the e_g states until they are crossed by E_F for Pd and Pt. A striking feature is the overall decrease of the DOS intensity and the similarity of the *T* and O PDOS especially for Pd and Pt. This is related to the larger quantum mixing between *T* and O whereby electrons are exchanged between *T* and O. From the calculations we find that the relative O(2*p*) occupation is increased from RuO_2 to PdO_2 and PtO_2. This charge exchange is in line with the increase of the covalent character of the bond.

Chemical bonding

To represent all four systems, the chemical bonding is illustrated in Fig. 4 using results of RhO_2, following the ECOV approach which merges both the Hamiltonian H_{ij} and the overlap S_{ij} analyses for pair interactions [19]. Along the *y* coordinate axis, negative,

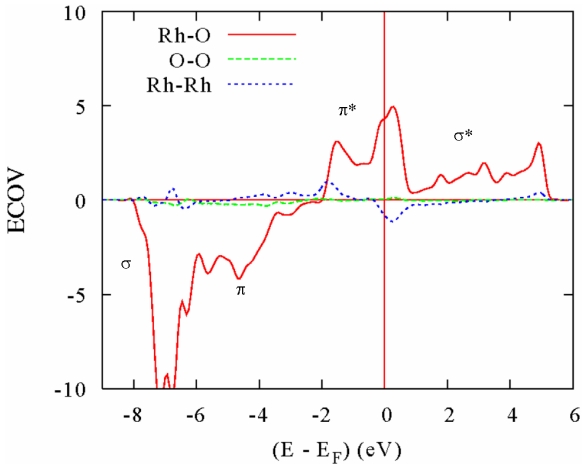

Fig. 4. Different interactions accounting for the site multiplicity of the ECOV criterion for rutile-type RhO_2.

positive and zero ECOV magnitudes point to bonding, antibonding and non-bonding interactions, respectively. It can be observed that the major pair interaction within the metal oxide systems arises from metal-oxygen bonding while only small contributions arise from *T*–*T* (Rh–Rh) and O–O bonding. The *T*–O bonding includes σ and π interactions involving the e_g and t_{2g} manifolds, respectively. This stabilizes the system within the valence band up to −2 eV. However, at the top of the valence band antibonding states appear with π^* bonding from t_{2g} manifolds; this is continued within the conduction band with σ^* interactions. This scheme of bonding resembles a classical molecular orbital (MO) diagram with σ and σ^* MO's much more separated, *i. e.* σ^* states higher in energy than weaker π and π^* MO's. This is like the diagram formerly described by Sorantin and Schwarz [12] for rutile-type oxides. It appears that at least part of the magnetic instability of the large DOS at E_F of these systems is due to antibonding states.

Conclusions

The oxides TO_2 (*T* = Ru, Rh, Pd, Pt) have been prepared through different routes. While RuO_2 also is found in nature, the synthesis of the other dioxides with *T* = Rh, Pd, Pt (not present in minerals) requires high oxygen pressures. Due to the strong covalence of the T^{4+}–O chemical bond with *T* = 4*d* and 5*d* transition metals, such dioxides are suitable candidates for theoretical investigations of their electronic band structures. First principles self consistent

computations providing a quantitative description of the band structure, the density of states DOS and the chemical bonding characteristics can be carried out in the framework of density functional theory. They allow for showing trends within the series of TO_2 oxides: The metallic character is mainly due to *d* states of the transition metal with different degrees of t_{2g}/e_g character. From energy positions of the bands and the DOS shapes the role of the metal and oxygen orbitals has been analyzed. There is an increasing rate of covalence within the series mainly through a broadening of the valence band (VB). A large DOS magnitude at the Fermi level was identified for the ruthenium oxide system and analyzed regarding on-site magnetic polarization of Ru(4*d*) states within a mean field theory of band ferromagnetism. The bonding within the VB is found to be predominantly of metal-oxygen character with low lying σ bonding and π-like bonding at higher energy, followed by π^* and σ^* states in an MO like manner.

Acknowledgements

Calculations were carried out on the main frame computers of the Université Bordeaux 1, M3PEC-Mésocentre (http://www.m3pec.u-bordeaux1.fr). This work was supported by the Deutsche Forschungsgemeinschaft and the European Science Foundation through the COST D30 programme.

[1] J. Zaanen, G. A. Sawatsky, J. W. Allen, *Phys. Rev. Lett*. **1985**, *55*, 418.
[2] D. B. Rogers, R. D. Shannon, A. W. Sleight, J. L. Gilson, *Inorg. Chem*. **1969**, *8*, 841; C. N. R. Rao, *Ann. Rev. Phys. Chem*. **1989**, *40*, 291.
[3] S. F. Matar, G. Campet, *J. Phys. Chem. Solids* **2007**, *68*, 31.
[4] C. E. Boman, *Acta Chem. Scand*. **1970**, *24*, 116; J. Haines, J. M. Léger, *Phys. Rev. B* **1993**, *48*, 13344.
[5] J. Haines, J. M. Léger, O. Schulte, *Science* **1996**, *271*, 629.
[6] D. Vrel, J. P. Petitet, X. Huang, T. Mashimo, *Physica B* **1997**, *239*, 9.
[7] O. Muller, R. Roy, *J. Less-Common Met*. **1968**, *16*, 129; R. D. Shannon, *Solid State Commun*. **1968**, *6*, 139.
[8] G. Demazeau, A. Baranov, R. Pöttgen, L. Kienle, M. H. Möller, R.-D. Hoffmann, M. Valldor, *Z. Naturforsch.* **2006**, *61b*, 1500.
[9] I. S. Shaplygin, G. L. Aparnikov, V. B. Lazarev, *Russ. J. Inorg. Chem*. **1978**, *23*, 488.
[10] K. J. Range, F. Rare, U. Klement, M. Heyns, *Mater. Res. Bull*. **1987**, *22*, 1541.
[11] L. F. Mattheiss, *Phys. Rev. B* **1976**, *13*, 2433; U. Lundin, L. Fast, L. Nordström, B. Johansson, J. M. Wills, O. Eriksson, *Phys. Rev. B* **1998**, *57*, 4979; R. R. Daniels, G. Margaritondo, C.-A. Georg, F. Lévy, *Phys. Rev. B* **1984**, *29*, 1813; S. F. Matar, G. Demazeau, J. Sticht, V. Eyert, J. Kübler. *J. Phys. I. France* **1992**, *2*, 315.
[12] P. I. Sorantin, K. Schwarz, *Inorg. Chem*. **1992**, *31*, 567.
[13] S. F. Matar, G. Demazeau, *Chem. Phys. Lett*. **2005**, *407*, 516; S. F. Matar, *Progr. Solid State Chem*. **2003**, *31*, 239.
[14] P. Honenberg, W. Kohn, *Phys. Rev*. **1964**, *136*, 864; W. Kohn, L. J. Sham, *Phys. Rev*. **1965**, *140*, A1133.
[15] A. R. Williams, J. Kübler, C. D. Gellat (Jr.), *Phys. Rev. B* **1979**, *19*, 6094; for a recent review see: V. Eyert, *Int. J. Quantum Chem*. **2000**, *77*, 1007.
[16] J. P. Perdew, S. Burke, M. Ernzerhof, *Phys. Rev. Lett*. **1996**, *77*, 3865.
[17] R. Hoffmann, *Angew. Chem*. **1987**, *99*, 871; *Angew. Chem. Int. Ed. Engl*. **1987**, *26*, 846.
[18] R. Dronskowski, P. E. Blöchl, *J. Phys. Chem*. **1993**, *97*, 8617.
[19] G. Bester, M. Fähnle, *J. Phys.: Condens. Matter* **2001**, *13*, 11541 and 11551.